

# Efficient spin polarised injection from manganites into carbon nanotubes

Luis E. Hueso<sup>1</sup>, José M. Pruneda<sup>2,3\*</sup>, Valeria Ferrari<sup>4</sup>, Gavin Burnell<sup>1</sup>, José P. Valdés-Herrera<sup>1,5</sup>, Benjamin D. Simons<sup>4</sup>, Peter B. Littlewood<sup>4</sup>, Emilio Artacho<sup>2</sup> & Neil D.

Mathur<sup>1</sup>

<sup>1</sup> *Department of Materials Science, University of Cambridge, Pembroke Street, Cambridge CB2 3QZ, UK*

<sup>2</sup> *Department of Earth Sciences, University of Cambridge, Downing Street, Cambridge CB2 3EQ, UK*

<sup>3</sup> *Institut de Ciencia de Materials de Barcelona, CSIC Campus U.A.B., 08193 Bellaterra, Barcelona, Spain*

<sup>4</sup> *Cavendish Laboratory, University of Cambridge, J J Thomson Avenue, Cambridge CB3 0HE, UK*

<sup>5</sup> *Nanoscience Centre, University of Cambridge, JJ Thomson Avenue, Cambridge CB3 0FF, UK*

\* Present address: *Department of Physics, University of California, Berkeley, CA 94720, USA*

The combination of molecular<sup>1</sup> and spin electronics<sup>2</sup> promises a new paradigm for functional materials via the manipulation of spin polarised electrons in novel environments. This is challenging because common electrode materials possess low spin polarisations, and efficient spin injection from one material to another is elusive. Consequently, only low-temperature magnetoresistance effects have been reported in carbon nanotubes contacted with cobalt<sup>3</sup>, and octanethiol or C<sub>60</sub> molecules contacted with nickel<sup>4,5</sup>. Here we integrate multiwall carbon nanotubes with epitaxial thin film electrodes of the ~100% spin polarised<sup>6</sup> manganite La<sub>2/3</sub>Sr<sub>1/3</sub>MnO<sub>3</sub>. Magnetocurrent effects persist up to 100 K, and a value of 37% at 5 K is recorded. This indicates a nanotube spin diffusion length in excess of 1 μm. Efficient spin injection between materials that are chemically and geometrically very different is surprising. We interpret our findings using density functional theory calculations that predict an energy barrier in the contact region and a manganite surface feature in the electronic density of states. The injection of highly spin polarised electrons from environmentally robust electrodes into molecules introduced ex-situ should inspire further developments in the nascent field of molecular spintronics.

Carbon nanotubes (CNTs) are molecules that possess unconventional electronic properties, and are in addition relatively robust and easy to manipulate. They have therefore been proposed for electronic applications, and successfully employed in proof-of-principle field effect transistors, quantum dots and logic gates<sup>7</sup>. The electronic spin states in CNTs are expected to be robust in view of weak spin-orbit coupling, but only small (~10%), low temperature magnetoresistance (MR) effects of different signs have been recorded in CNTs contacted with nearby (e.g. 200 nm) ferromagnetic electrodes<sup>8-10</sup>. Specific materials combinations might or might not permit efficient spin injection. For example, spin injection between cobalt and copper forms the basis of modern disk-drive read heads<sup>11</sup>, but spin injection between ferromagnetic metals and semiconductors appears poor<sup>12</sup>. In conventional electronics ohmic contacts tend to be favoured. However, for any given materials combination, the presence of an energy barrier can enhance spin injection, as argued in bulk systems<sup>13-15</sup>.

We report here magnetoresistance effects in CNT devices using ferromagnetic metallic electrodes of the manganite  $\text{La}_{2/3}\text{Sr}_{1/3}\text{MnO}_3$  (LSMO). At low temperatures, this pseudo-cubic perovskite oxide possesses ~100% spin polarised conduction electrons<sup>6</sup>, whereas the spin polarisation of elemental ferromagnets is less than 40%<sup>16</sup>. Moreover, since LSMO is an oxide, it displays environmental stability so that molecules may be introduced ex-situ.

Deterministic synthesis routes do not deliver optimal quality manganite–carbon nanotube heterostructures because of the conflicting oxygen ambient growth requirements. We therefore pursued a non-deterministic strategy that involved dispersing commercial 20 nm diameter multiwall carbon nanotubes onto micron scale electrodes that were lithographically defined from optimised LSMO films (Fig. 1 and Methods). Each working device comprised a single nanotube spanning adjacent electrodes whose magnetizations could be switched independently by an external magnetic field. This switching was inferred from similar and reproducible MR effects seen in 4 devices, in which we presume that magnetic impurities in the CNT are absent. These 4 devices formed a subset of the 12 devices that showed similar and reproducible current-voltage ( $I$ - $V$ ) characteristics, and these 12 devices formed a subset of the 60 devices that showed some form of electrical conductivity. Representative results were unaffected by the introduction of silica between the electrodes to prevent the nanotubes from sagging.

A typical working device shows zero-field electrical characteristics (Fig. 2) in which the low temperature, low bias conductance is an order of magnitude smaller than similar Pd-CNT-Pd devices<sup>17</sup>. Referring to the 5K data, one can identify an upturn at 210 mV which could reflect a barrier or feature in the density of states. Modelling this feature is not appropriate since our back-to-back LSMO-CNT junctions preclude fitting the data at low

bias. Our main result is a pronounced and bistable low-field MR, i.e. a resistance that is low (high) when the magnetization of the electrodes is parallel (antiparallel). This behaviour results from the half-metallic character of our electrodes, but we note that quantum mechanical tunnelling across the interfaces in our devices is not required. We present the bistable MR in Fig. 3a as a magnetocurrent (MC) given that our  $I$ - $V$  curves are non-linear. The low temperature, low bias limit of MC=37% suggests a lower bound for the CNT spin-diffusion length<sup>3</sup>  $l_S = 1 \mu\text{m}$ , assuming that our electrodes separated by 1.5  $\mu\text{m}$  are 100% spin polarised. This value of  $l_S$  is an order of magnitude improvement over previous CNT measurements<sup>3,8</sup>.

An increase of bias or temperature reduces the peak MC (Fig. 3b) but does not qualitatively alter the dependence of MC on applied magnetic field  $B$ . At 5 K, a zero bias anomaly associated with spin-wave excitations<sup>18</sup> could not be fully resolved due to the limitations of our low-level current detection capabilities. The plateau in peak MC extending up to 110 mV may be associated<sup>18</sup> with tunnelling from majority spin states in the source electrode to minority spin states in the drain electrode. This plateau arises at a higher bias in LSMO tunnel junctions with SrTiO<sub>3</sub> barriers<sup>18</sup>, possibly because here the material between the LSMO electrodes possesses a very different chemistry and aspect ratio. Above 110 mV, the peak MC falls such that it is highly suppressed when the bias exceeds the observed feature of  $\sim 200$  mV.

The temperature dependence of the peak MC at 25 mV decreases monotonically to zero at 100 K, even though the Curie temperature  $T_C$  of the electrodes is 350 K. Similar behaviour has been observed in manganite tunnel junctions where the bistable MC is lost at around  $0.5T_C$ <sup>19</sup>. Although we cannot independently resolve any thermal suppression of  $l_S$ , a simple explanation of the thermal suppression of the MC is that the spin polarisation of the electrodes is reduced at interfaces due to a loss of the bulk symmetry<sup>20</sup> and structural imperfections. Specifically, density functional theory (DFT) calculations (Methods) find a LSMO surface state, and predict a transfer of 0.1 electrons per  $\text{\AA}$  from the CNT to the LSMO such that the local doping and therefore the local  $T_C$  of the latter is reduced.

We now discuss the origin of the 200 mV feature that is observed (Fig. 2) and appears to be important for MC (Fig. 3b). One expects the LSMO-CNT interface to dominate device resistance, especially since SEM observations suggest an effective area that is only 50% of the apparent area due to incomplete contact. Our DFT calculations support this picture because they show a weak electronic contact at the interface, clearly illustrated by the energy barrier shown in the inset of Fig. 4. The height of the barrier represents an effective upper bound on its experimental counterpart, given that any lower barrier arising due to heterogeneity of the contact will channel the conduction.

The DFT calculations show an energy shift of  $\sim$ 200 meV between states in a CNT on LSMO, and states in an isolated CNT (Fig. 4a). This indicates that in our device one may expect an energy shift of this magnitude associated to the interface within the CNT that lies at the edge of the LSMO contact (plane X, Fig 1c). This shift is related to the charge transfer of 0.1 electrons/ $\text{\AA}$  from the CNT to the LSMO mentioned above. The similarity between the value of this energy shift and the observed  $I$ - $V$  feature (Fig. 2) is striking. It would thus be tempting to assume a semiconducting CNT in which a Schottky barrier forms between the suspended and supported regions, especially considering that the CNT possesses a cross-sectional area that is at least an order of magnitude smaller than the contact area such that any feature in it has the potential to dominate. However, the current understanding of the electronic properties of CNTs preclude this interpretation, given that the optical gap of 40 meV for a 20 nm semiconducting tube<sup>7</sup> suggests that the quasiparticle gap is too small to sustain such a barrier. Instead, the observed 200 meV feature could be a density of states effect. Indeed, the predicted LSMO surface state displays a strong energy dependence around 200 meV below the Fermi level that is absent in the bulk (Fig. 4b). This surface state introduces minority spin states at the Fermi level, which would reduce the theoretical upper bound of the MC to 80%, and therefore slightly increase the lower bound of  $l_s$  to 1.8  $\mu\text{m}$ .

This work provides direct evidence for spin coherence in CNTs. We anticipate that our findings will inspire spintronic studies of other molecules introduced ex-situ onto nearby LSMO electrodes. Ultimately this work could therefore lead to improved functionality in nanoscale electronic circuits. Specifically, it may impact quantum computing. For example, a CNT carrying coherent spins could act as a turnstile device that delivers a single spin to specific location, e.g. as an interconnect for qubits.

## METHODS

**Experimental.** Epitaxial LSMO thin films were grown on closely lattice matched orthorhombic  $\text{NdGaO}_3$  (001) substrates by pulsed laser deposition with a KrF excimer laser (248 nm, 1 Hz,  $2.5 \text{ Jcm}^{-2}$ , 775°C, 15 Pa  $\text{O}_2$ , target-substrate distance = 8 cm). The films display step-terrace growth, and possess in-plane uniaxial magnetocrystalline anisotropy in the orthorhombic [100] direction. Below 360 K the films are ferromagnetic ( $3.6 \mu_B/\text{Mn}$  at 10 K), and on cooling the resistivity decreases to  $\sim$ 60  $\mu\Omega\text{cm}$  at 10 K. Using conventional photolithography, electrode tracks (width 1-4  $\mu\text{m}$ , separation 1.5  $\mu\text{m}$ ) were defined perpendicular to [100]. Multiwall carbon nanotubes of diameter  $\sim$ 20 nm grown by arc-discharge (Iljin Nanotech Co. Ltd., Korea) were subsequently dispersed from a 1,2-dichloroethane solution. A SEM was used to confirm the presence of a single nanotube running

between adjacent electrodes that showed electrical conductivity in a probe station. Aluminium wire bonds were ultrasonically attached to contact pads at the end of the tracks. Electrical transport measurements were made in a continuous-flow He cryostat using a constant voltage source.

**Theoretical.** First-principles electronic-structure calculations were performed within the density-functional-theory (DFT) framework<sup>21</sup> in the spin-polarised generalized-gradient approximation, using the SIESTA method<sup>22</sup>. Further details on the performance of the method for LSMO can be found elsewhere<sup>23</sup>. The MnO<sub>2</sub>-terminated (001) surface of LSMO was described by a 23-layer slab of LSMO, in which one third of the La atoms were replaced by Sr<sup>23</sup>. A (6,6) single-wall CNT was put onto the LSMO surface in a commensurate arrangement in which 3 unit cells of the CNT were laid along the (100) direction on a 4x2 lateral supercell of LSMO. The mismatch strain is 5 %. The position of the CNT on the surface was obtained by relaxing the mutual DFT force. Even though experiments were performed on multiwall nanotubes which are arguably better described in the graphitic limit, we have nevertheless considered a nanotube, since the dimensionality greatly affects the contact resistance. The value for the charge transfer may change, but the qualitative picture emerging from the calculations remains. The energy barrier obtained between LSMO and CNT should not change appreciably with the type of CNT.

**Acknowledgements.** We thank G.A.J. Amaratunga, M. Buitelaar, L. Brey, M.J. Calderón, Seung Nam Cha, M. Chhowalla, D.-J. Kang, and N. Spaldin. This work was funded by the UK EPSRC, NERC, BNFL, The Royal Society, Spanish MEC (JMP), Donostia International Physics Center (EA) and the EU.

1. Joachim, C., Gimzewski, J.K. & Aviram, A. Electronics hybrid-molecular and monomolecular devices. *Nature* **408**, 541-548 (2000).
2. Wolf, S.A., Awschalom, D.D., Buhrman, R.A., Daughton, J.M., von Molnar, S., Roukes, M.L., Chtchelkanova, A.Y. & Treger, D.M. Spintronics: A spin-based electronics vision for the future. *Science* **294**, 1488-1495 (2001).
3. Tsukagoshi, K., Alphenaar, B.W. & Ago, H. Coherent transport of electron spin in a ferromagnetically contacted carbon nanotube. *Nature* **401**, 572-574 (1999).
4. Petta, J.R., Slater, S.K., Ralph, D.C. Spin-dependent transport in molecular tunnel junctions. *Phys. Rev. Lett.* **93**, 136601 (2004).
5. Pasupathy, A.N., Bialczak, R.C., Martinek, J., Grose, J.E., Donev, L.A.K., McEuen, P.L. & Ralph, D.C. The Kondo effect in the presence of ferromagnetism. *Science* **306**, 86-89 (2004).

6. Park, J.-H., Vescovo, E., Kim, H.-J., Kwon, C., Ramesh, R. & Venkatesan, T. Direct evidence for a half-metallic ferromagnet. *Nature* **392**, 794-796 (1998).
7. Dresselhaus, M.S., Dresselhaus G. & Avouris, Ph. (eds) *Carbon Nanotubes* (Springer, Berlin, 2001).
8. Zhao, B., Mönch, I., Vinzelberg, H., Mühl, T. & Schneider, C.M. Spin-coherent transport in ferromagnetically contacted carbon nanotubes. *Appl. Phys. Lett.* **80**, 3144-3146 (2002).
9. Jensen, A., Hauptmann, J.R., Nygård J. & Lindelof, P.E. Magnetoresistance in ferromagnetically contacted single-wall carbon nanotubes. *Phys. Rev. B* **72**, 035419 (2005).
10. Sahoo, S., Kontos, T., Schönenberger, C. & Sürgers, C. Electrical spin injection in multiwall carbon nanotubes with transparent ferromagnetic contacts. *Appl. Phys. Lett.* **86**, 112109 (2005).
11. Maekawa, S. & Shinjo, T. (eds) *Spin dependent transport in magnetic nanostructures* (London, Taylor & Francis, 2002).
12. Tang, H.X., Monzon, F.G., Jedema, F.J., Filip,A.T., van Wees, B.J. & M. L. Roukes in *Semiconductor spintronics and quantum computation* (eds Awschalom, D., Loss, D. & Samarth, N.) 35-95 (Springer Verlag,Berlin, 2002).
13. Schmidt, G., Ferrand, D., Molenkamp, L.W., Filip, A.T. & van Wees, B.J. Fundamental obstacle for electrical spin injection from a ferromagnetic metal into a diffusive semiconductor. *Phys. Rev. B* **62**, 4790-4793 (2000).
14. Rashba, E. Theory of electrical spin injection: tunnel contacts as a solution of the conductivity mismatch problem. *Phys. Rev. B* **62**, 16267-16270 (2000).
15. Fert, A. & Jaffrè, H. Conditions for efficient spin injection from a ferromagnetic metal into a semiconductor. *Phys. Rev. B* **64**, 184420 (2001).
16. Meservey, R. & Tedrow, P.M. Spin-polarized electron tunneling. *Phys. Rep.* **238**, 173-243 (1994).
17. Hueso, L.E., Burnell, G., Prieto, J.L., Granja, L., Bell, C., Kang, D.-J., Chhowalla, M., Cha, S.N., Jang, J.E., Amaratunga, G.A.J. & Mathur, N.D. Electrical transport between epitaxial manganites and carbon nanotubes. <http://www.arXiv.org/cond-mat/0511259>.
18. Bowen, M., Barthélémy, A., Bibes, M., Jacquet, E., Contour, J.-P., Fert, A., Ciccacci, F. Duò, L. & Bertacco, R. Spin-polarized tunnelling spectroscopy in tunnel junctions with half-metallic electrodes. *Phys. Rev. Lett.* **95**, 137203 (2005).
19. Jo, M.-H., Mathur, N.D, Todd, N.K. & Blamire, M.G. Very large magnetoresistance and coherent switching in half-metallic manganite tunnel junctions. *Phys. Rev. B* **61**, 14905-14908 (2000).

20. Calderón, M.J, Brey, L. & Guinea, F. Surface electronic structure and electronic properties of doped manganites. *Phys. Rev. B* **60**, 6698-6704 (1999).
21. Kohn, W. & Sham, L. J. Self-consistent equations including exchange and correlations effects. *Phys. Rev.* **140**, 1133-1138 (1965).
22. Soler, J. M., Artacho, E., Gale, J. D., García, A., Junquera, J., Ordejón, P. & Sánchez-Portal, D. The SIESTA method for ab initio order-N materials simulation. *J. Phys.: Condens. Matt.* **14**, 2745-2779 (2002).
23. Ferrari, V., Pruneda, J. M. A. & Artacho E. Density Functionals and half-metallicity in  $\text{La}_{2/3}\text{Sr}_{1/3}\text{MnO}_3$ . <http://www.arXiv.org/cond-mat/0511432>.

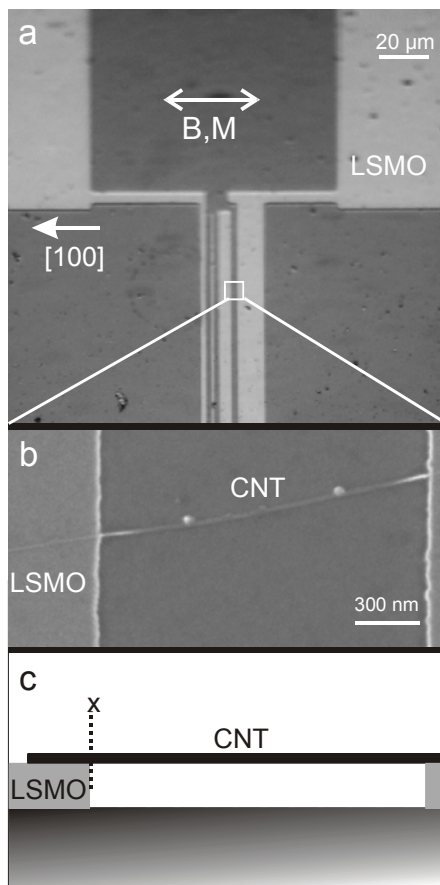


**Figure 1 | LSMO-CNT-LSMO.** **a**, optical micrograph of four variable width LSMO electrodes, and two of the four associated contact pads. In electrically conducting devices, two adjacent electrodes were connected by an overlying CNT, e.g. in the boxed region. Magnetic fields **B** were applied along the orthorhombic [100] direction in which the magnetization **M** is expected to lie due to uniaxial magnetocrystalline anisotropy. **b**, SEM image of a CNT running between LSMO electrodes. **c**, schematic side view of **b** with the plane through the CNT at the edge of the LSMO electrode denoted X.

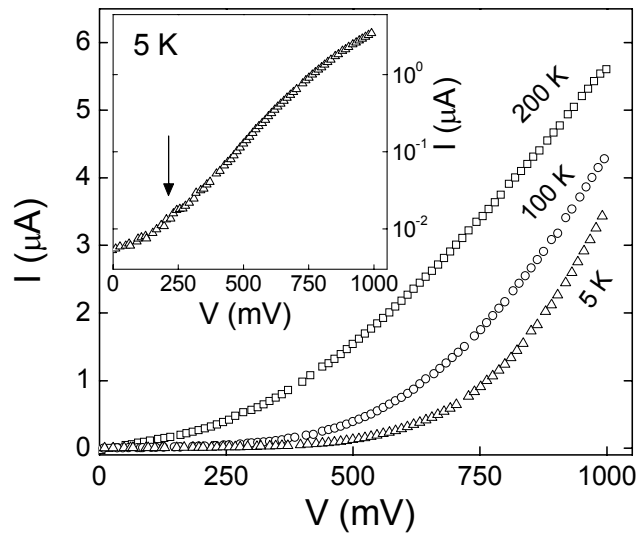


**Figure 2 | Zero-field symmetric  $I$ - $V$  characteristics for a typical LSMO-CNT-LSMO device.** Main panel, data at selected temperatures in the range 5–200 K. Device symmetry precludes rectification. Inset, a semi-logarithmic plot of the 5 K data reveals a maximum in curvature around 210 mV. All data correspond to the low resistance state associated with the parallel magnetic electrode configuration discussed in Fig. 3.

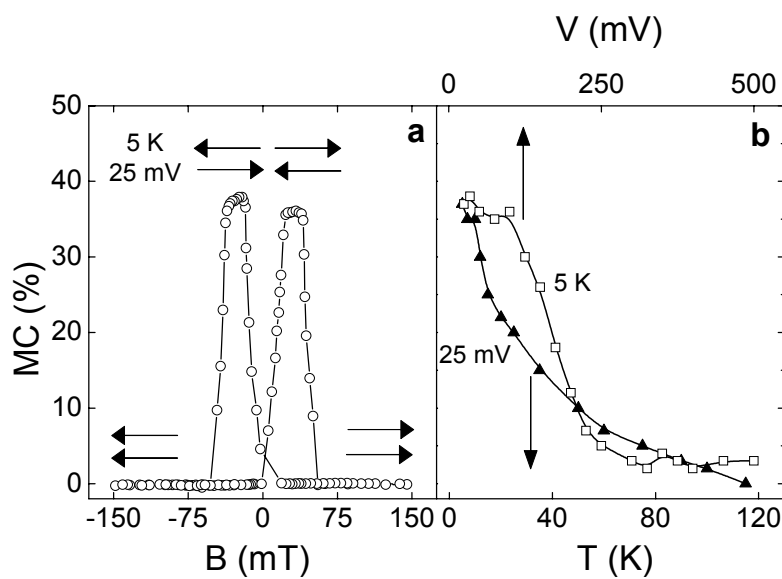


**Figure 3 | Low-field magnetocurrent.** Left panel, data ( $\circ$ ) taken at low temperature and bias show the classic two state low-field response associated with the switching magnetizations of the electrodes (arrows indicate their relative orientations).  $MC(B)=100\times(I(0)-I(B))/I(0)$ , where  $I(B)$  denotes the current  $I$  in applied magnetic field  $B$ . Data were averaged over 25 cycles and the lines were generated accordingly. Right panel, Peak MC as a function of bias at low temperature ( $\square$ ), and as a function of temperature at low bias ( $\blacktriangle$ ).

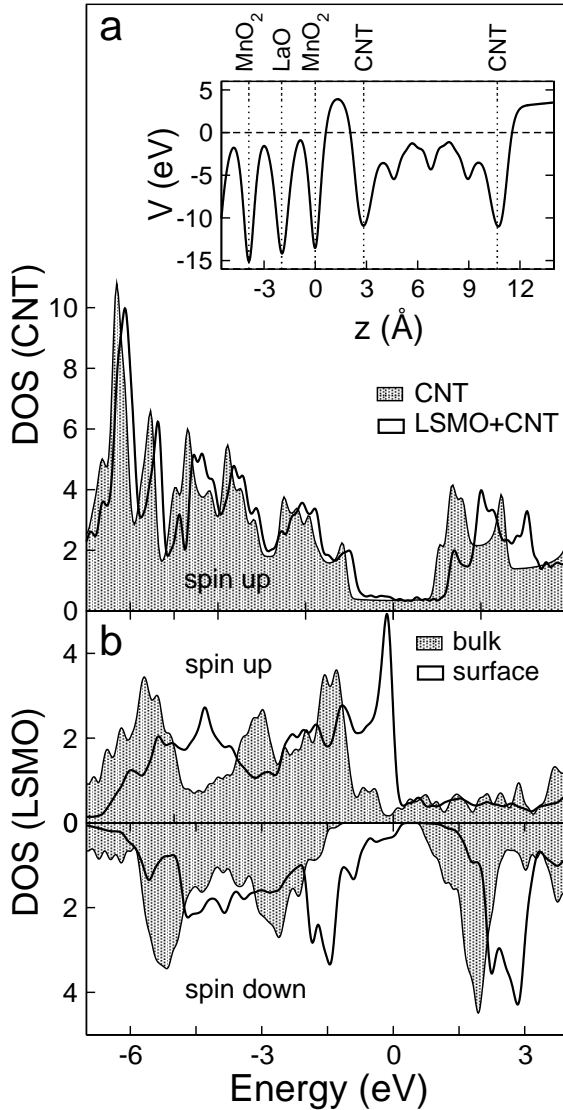


**Figure 4 | Density functional theory calculations.** Projected density of states (DOS) on **a**, the basis functions of an isolated CNT (shaded), and a CNT lying on LSMO (unshaded). **b**, the projected DOS onto the first  $\text{MnO}_2+(\text{La},\text{Sr})\text{O}$  layer of the LSMO slab (unshaded) shows a feature near 200 meV that is absent in bulk LSMO (shaded). Fermi levels aligned at  $E=0$ , only up spins shown in **a**, since up-down differences in the CNT DOS are barely visible at this scale (there is a net spin polarisation of +0.01 electrons/Å). **Inset**, the Kohn-Sham potential seen by electrons in the vicinity of the LSMO/CNT interface. It has been integrated for each value of  $z$  (normal to the LSMO surface) in the rectangle defined by the projection of the CNT onto the  $x$ ,  $y$  plane. The potential origin has been chosen at the Fermi level (horizontal dashed line). Vertical dotted lines indicate the nuclear positions of the atomic layers of LSMO, and of the limits of the CNT.